ACS ENGINEERING Au
AN OPEN ACCESS JOURNAL OF THE AMERICAN CHEMICAL SOCIETY

pubs.acs.org/engineeringau
Article

Electrodialysis for the Recovery of Acetate from Microbial Electrosynthesis Effluents

Santiago Martínez Sosa,* Qingdian Shu, Michele Tedesco, Hubertus V.M. Hamelers, Pau Farràs, and Paolo Dessì

Cite This: https://doi.org/10.1021/acsengineeringau.5c00110
Read Online

ABSTRACT: Microbial electrosynthesis (MES) is a promising bioelectrochemical technology for converting CO_2 into value-added products. However, downstream processing remains a major constraint for its application at larger scales. There is limited understanding of which separation technologies can be effectively integrated with MES effluents, and how key operating conditions impact on the product recovery and energy efficiency. This study assesses the use of electrodialysis (ED) as a solvent-free downstream separation process for acetate recovery from a multicomponent simulated MES effluent. The effects of operating pH (3, 5.5, and 7.5), applied current density (1.9, 3.8, 9.5, and 15.0 mA cm^{-2}), and operation mode (continuous or fed-batch) were investigated. The highest acetate titer (13.73 ± 1.65) in the concentrate stream was reached at pH 5.5, a current density of 1.9 mA cm^{-2}, and under fed-batch operation. Ion competition was identified as the primary limiting factor, with preferential Cl^- transport, which reduced the Coulombic efficiency of acetate transport to 34.97 ± 0.63%. Under these conditions, the ED system recovered 1.12 ± 0.03 kg of acetate per kWh, corresponding to approximately 5% of the total energy demand associated with MES production. Overall, this study provides quantitative guidance on the optimization of electrodialysis as a recovery technology from a simulated MES effluent as a low-energy downstream solution for MES systems, helping to address key bottlenecks faced by this technology.

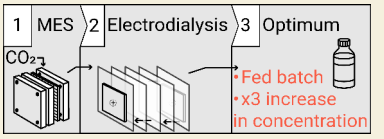

KEYWORDS: *electrodialysis, operation parameters, carboxylic acids, downstream, bioelectrochemical system*

1. INTRODUCTION

Human development is directly tied to resource consumption, inevitably linking economic growth to environmental degradation. This degradation is evident in the relentless consumption of energy, overexploitation of natural resources, and extensive waste generation.[1] Notably, fossil fuel combustion remains the largest source of greenhouse gases, predominantly carbon dioxide (CO_2), which has reached a record atmospheric concentration of 423 ppm as of July 2024,[2] contributing to more than 60% of the global warming phenomenon.[3] Thus, urgent action is imperative to reduce these emissions, with stricter policies and the development of technology that can prevent further catastrophes, as outlined in the Paris Agreement.[4]

A fundamental shift in both producer and consumer behavior is needed, and the circular economy (CE) emerges as a transformative model, aiming to decouple economic growth from material consumption in contrast with traditional linear economic models.[5] Within this model, green chemical production through carbon capture and utilization (CCU) technology is a promising pathway to synthesize green chemicals and prevent pollution,[6] mitigating global emissions and alleviating the carbon footprint of carbon-intensive industries.

Bioelectrochemical systems (BESs) can convert energy into chemical products or vice versa. Among these processes, microbial electrosynthesis (MES), in which bacteria are used for electricity-driven CO_2 reduction, is one of these CCU technologies developed to produce value-added chemicals.[7,8] Along with other CCU processes, BES offers an alternative to conventional petrochemical-derived chemical production, reducing reliance on fossil fuels and minimizing environmental impact. By leveraging these processes, the chemical industry could transition to a circular carbon economy, where CO_2 is seen as a resource rather than a burden.[9]

As in any production process, MES can be divided into upstream (chemical production from CO_2) and downstream (concentration and purification steps to reach a final product). Downstream processing is critical to ensure product quality and marketability. However, it poses significant challenges, often accounting for up to 50% of total production costs.[10] Downstream processing can be particularly difficult in MES-producing acetic acid,[11] which, due to its high solubility in water, is difficult to separate from aqueous solutions. Depending on the characteristics of the product of interest, treatment methods such as distillation and extraction are commonly employed in chemical processing downstream.[12] While effective, these methods have limitations, including high-energy consumption,

Received: November 26, 2025
Revised: February 20, 2026
Accepted: February 23, 2026

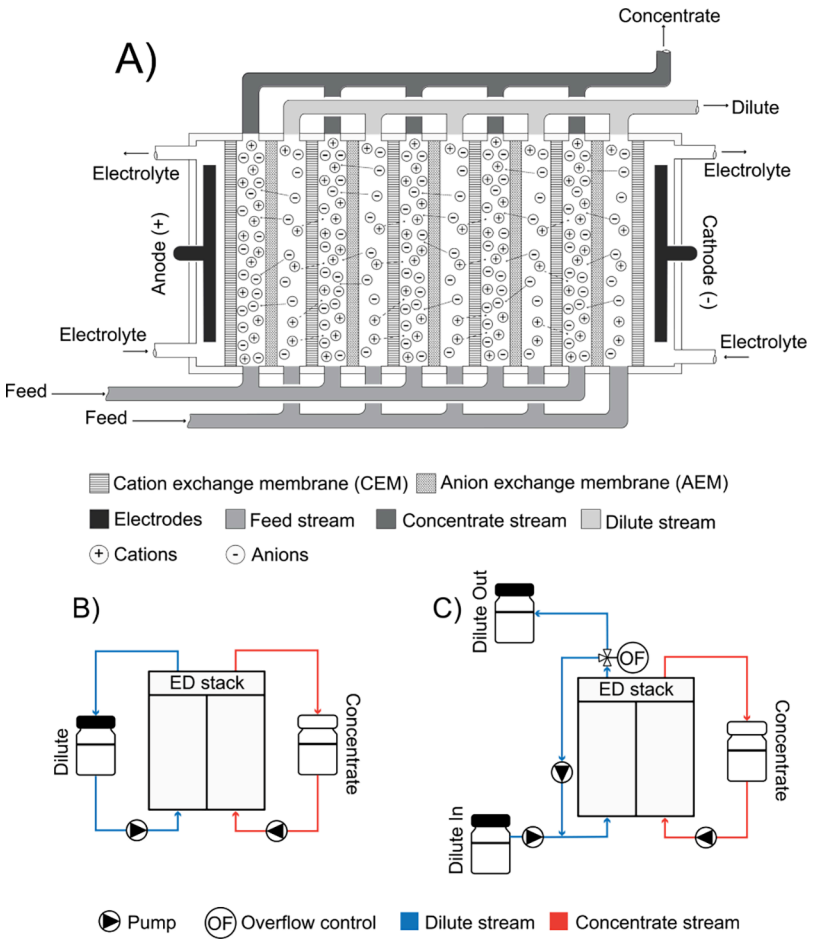

Figure 1. (A) Schematic representation of the ED stack used in this study, including membrane location and flow compartments. (B) Experimental setup used for the batch and fed-batch operation. (C) Experimental setup used for continuous operation with a continuous supply (dilute in) and removal (dilute out) of solution.

contamination of the products with adsorbents, and the use of nonbiocompatible solvents, which can reduce their viability for green chemical production.[13]

In bioprocesses, in-line product separation offers advantages, as it allows control over product accumulation and the consequent inhibition of the microbial community. Saboe et al.[14] developed a model combining liquid−liquid extraction with distillation for the *in situ* extraction of biotic, short- and medium-chain carboxylic acids. However, using toxic solvents can affect the microorganisms, which threatens the process. Other studies have proposed in-line extraction of carboxylic acids in BES. Matemadombo et al.[15] proposed a model for simultaneously producing and extracting acetic acid, reaching concentrations of 0.24 g L^{-1} in the concentrated stream. On the other hand, Gildemyn et al.[16] proposed a three-chamber BES system capable of synthesizing and extracting acetic acid, reaching a concentration of 13.5 g L^{-1}. The latter demonstrate the potential of electrically driven processes for the recovery of BES products. However, the addition of a third chamber and an extra membrane inevitably increase the ohmic losses of the cells.

Since MES cells are usually operated at pH above the pK_a of acetic acid, several technologies such as anion-exchange resins, membranes, and ionic liquids have been used for its extraction in the ionic form.[17] Among these technologies, membrane-based systems such as electrodialysis (ED) have reached a high level of development.[18] Although ED technology has been applied for various purposes such as the production of chemicals from seawater brine or the recovery of carboxylic acids from fermentation broths,[19,20] several technical challenges, such as the selectivity of competing ions, scaling, and long-term stability in specific applications still limit its widespread usage.[21]

ED has been previously combined with MES.[22] In that study, acetic acid was produced from CO_2 in a hybrid system, including an electrolyzer and a bubble column reactor. ED was integrated to such a system to enable in-line product recovery, resulting in a production rate increase from 2 to 4.32 g L^{-1} day^{-1}, with 84% Coulombic efficiency, and product accumulation up to 98.1 g L^{-1}. However, such ED system only included a single AEM/CEM pair, while a multistack ED system is a preferred technology for scale-up in terms of extraction rates and energy consumption. Furthermore, the combined system was operated under a single fixed set of parameters, without optimizing the ED operation considering crucial parameters such as current density and pH. Finally, the faith of competing anions in the system (e.g., Cl^-), which could widely affect the applicability of this method to MES effluents, was not assessed.

In this context, the objective of this work was to investigate a laboratory-scale ED system as a downstream process for acetate recovery from a simulated MES effluent that mimics the MES process output previously obtained by Dessì et al.[23] This study provides the first systematic evaluation of the effects of operating parameters (pH, current density, and operation regimen) on the

https://doi.org/10.1021/acsengineeringau.5c00110
ACS Eng. Au XXXX, XXX, XXX−XXX

Table 1. Operating Parameters of the 10 ED Experiments Performed

Parameter under study	blank	pH			current density				operation mode	
Experiment code	E1[a]	E2	E3	E4	E5	E6	E7	E8	E9	E10
mode[b]	B	B	B	B	B	B	B	B	C	FB
pH	7.3	3	5.5	7.5	5.5	5.5	5.5	5.5	5.5	5.5
CH_3COOH (g L^{-1})	0	5	5	5	5	5	5	5	5	5
current density (A m^{-2})	1.9	1.9	1.9	1.9	1.9	3.8	9.5	15.0	1.9	1.9
linear flow velocity (cm h^{-1})	10.2	10.2	10.2	10.2	30.5	30.5	30.5	30.5	10.2	10.2
Concentrate initial volume (mL)	300	300	300	300	300	300	300	300	700	700
dilute initial volume (mL)	300	300	300	300	300	300	300	300	5000	700
electrolyte volume (mL)	300	300	300	300	300	300	300	300	700	700
influent flow rate (mL min^{-1})									4.2	
NaOH added (g L^{-1})			2.4	3.5	2.4	2.4	2.4	2.4	2.4	2.4

[a]The first experiment conducted served as a blank, with a feed solution containing all the components previously mentioned except for acetic acid, to establish a baseline for ion transportation within the ED stack. [b]B: Batch, C: continuous, and FB: fed-batch.

performance of an ED stack for the concentration of acetic acid produced in a MES system, in terms of product recovery and electrical energy consumed.

2. MATERIALS AND METHODS

2.1. Electrodialysis Stack Setup

The ED stack used in this study consisted of five cell pairs (Figure 1A), resulting in a total volume of 50 cm^3. Each cell pair was equipped with a 100 cm^2 homogeneous cation exchange membrane (CEM-Type 10, Fujifilm, The Netherlands) and a 118 cm^2 homogeneous anion-exchange membrane (AEM-Type 10, Fujifilm, The Netherlands). An additional CEM was incorporated between the last cell pair and the anode to complete the stack. Membranes were separated using silicone gaskets and woven polymeric (nitrile) spacers (500 μm, SEFAR 07-200/43, Switzerland), which created channels for the concentrated and dilute streams. The electrodes consisted of titanium mesh (9.8 × 9.8 cm, Magneto Special Anodes BV, The Netherlands), coated with Ir/Ru (anode) and platinum (cathode). The entire ED stack was enclosed between two poly(methyl methacrylate) (PMMA) end plates (21 × 21 × 2.5 cm), which sealed the system by applying pressure through screws.

A synthetic solution containing the following (in g L^{-1}): KH_2PO_4 (0.33), K_2HPO_4 (0.45), NH_4Cl (1.0), KCl (0.1), $MgSO_4 \cdot 7H_2O$ (0.2), $NaHCO_3$ (0.12), NaCl (5), and CH_3COOH (5) was prepared. This composition was selected to simulate the outlet stream of a previously operated MES cell-producing acetic acid from CO_2 under moderate saline conditions.[23] The synthetic solution was used as the feed solution for the ED stack. Additionally, a solution of sodium sulfate (Na_2SO_4) with a concentration of 6.18 g L^{-1} (referred to as "electrolyte solution") was supplied to the electrode chambers to rinse them and maintain the sodium ion concentration at the same level as in the feed solution. This solution was circulated at a flow rate of 10.17 cm h^{-1}.

The feed solution was recirculated at a controlled flow rate to achieve the required linear flow velocity (refer to Table 1) using peristaltic pumps (Masterflex 77202-60, Methronom Applikon BV, The Netherlands) and polyethylene tubing. The electrode rinse solution was recirculated in a single container for all experiments, while independent containers were used for the concentrate and dilute streams (Figure 1B).

The current applied to the system was regulated using a power supply (ES 030-5, Delta Electronika BV, The Netherlands). Conductivity and pH were monitored using online probes (Memosens CLS82D and Memosens CPS11E, Endress+Hauser BV, The Netherlands) for the concentrate and dilute streams, respectively. All probes were connected to a data transmitter box (CM444, Endress+Hauser BV, The Netherlands) and a data logger (Memograph M RSG40, Endress +Hauser BV, The Netherlands). Saturated calomel electrodes (SCEs) were used to measure the electrode potentials (+0.241 V vs NHE, QM712X, QiS-Prosense BV, The Netherlands), positioned at the inlet of the electrode compartments.

2.2. ED Stack Operation

This study was carried out in 10 ED experiment sets (Table 1). Unless otherwise stated, the reported values represent the mean value of triplicate experiments with the corresponding standard deviation. All of the experiments were performed at room temperature. When necessary, the pH of the feed solution was adjusted using NaOH pellets (≥97.0%, Fisher Scientific). Before applying current to the system, the feed solution was circulated to ensure complete submersion of the sensor probes and to eliminate any air bubbles in the lines that could affect the experimental outcomes. After the power source was activated, relevant parameters were recorded every minute throughout the experiments. All experiments were conducted under a constant current regime and were stopped when the conductivity of the dilute stream decreased to approximately 1 mS cm^{-1}, indicating ion depletion. The volume of the dilute, concentrate, and electrolyte solutions was measured at the beginning and end of each experiment to account for water transport between streams.

The recirculation flow velocity in the ED stack was selected to ensure electrolyte mixing, preventing constrains such as concentration polarization or limited mass transfer.[24]

The current density range was selected to allow fast enough ion migration, avoiding long time operation with low conductivity in the dilute stream, but avoiding too high current that may result in concentration polarization.[24]

The experiments were conducted at pH 3, 5.5, and 7.5 (Table 1). pH 5.5 (E3) was selected to simulate the MES effluent obtained in a previous study.[23] On the other hand, pH 3 (E2) and pH 7 (E4) were selected to evaluate the ED-based extraction process in the prevalence of undissociated or dissociated acetic acid form, respectively.

Finally, the selection of operating modes was made based on process manufacturing literature stating that switching from batch to fed-batch or continuous operation affect the system's productivity and efficiency.[24,25]

The batch experiments (E1−8, Table 1) were conducted using the configuration shown in Figure 1B. For the continuous experiment (E9, Table 1), an overflow control system was incorporated to regulate the dilute stream outlet flow, while individual peristaltic pumps controlled the inlet (0.41 cm h^{-1}) and recirculation (10.17 cm h^{-1}) flow velocities (Figure 1C). The concentrate stream was maintained under recirculation (10.17 cm h^{-1}), as in the batch experiments. The outlet of the dilute stream was collected in a separate container for the analysis.

In the fed-batch experiment (E10, Table 1), the same configuration as that of the batch experiments was used. However, when the stop conditions were reached, the power supply was turned off, and the dilute solution was replaced with a fresh solution for the subsequent batch while maintaining the same solution in the concentrate and electrolyte containers. Both the continuous and fed-batch experiments were conducted for 18 h. This operating time allowed to reach steady-state conditions in the dilute stream of the continuous system (E9). The

https://doi.org/10.1021/acsengineeringau.5c00110
ACS Eng. Au XXXX, XXX, XXX−XXX

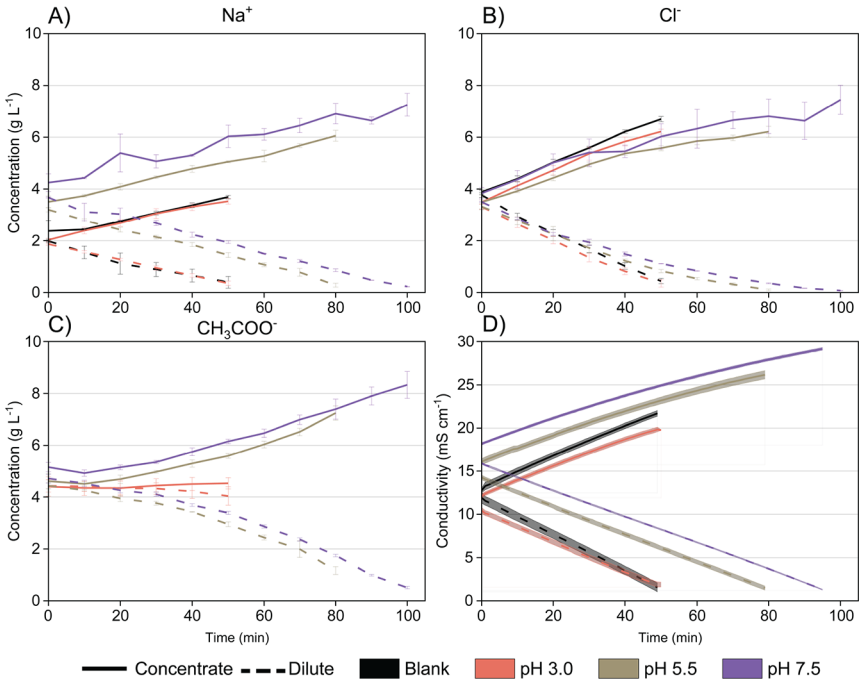

Figure 2. Effect of operating pH on the ion concentration variation in the ED streams as a function of time for (A) Na^+, (B) Cl^-, and (C) CH_3COO^- for experiments E1−E4. (D) Effect of operating pH on the conductivity variation of the ED streams over time for experiments E1−E4. Differences in the initial Na^+ concentration arise from NaOH addition for pH adjustment.

same operating time was applied to fed-batch operation (E10) to allow comparison.

In the batch experiments, concentrate and dilute samples were collected at the beginning and at regular time intervals throughout the experiments depending on the applied current density. The sampling time was set to 10 min for an applied current density of 1.9 mA cm^{-2}, while at higher current densities, the sampling time was adjusted to ensure at least five samples were collected during each experiment. For the continuous experiment, samples were taken every hour during the initial hours of operation, followed by a final sample after 18 h. For the fed-batch experiment, samples were collected every 30 min.

A total of 30 experiments were performed in this study. The variance was assessed by performing each experiment in triplicate. The membranes were never replaced during the experiments, but the system was regularly rinsed with DI water after each experiment. Despite this, no indicators of performance loss, such as stack voltage variation, system resistance, or flow issues, were detected.

2.3. Sample Analysis and Calculations

The composition of liquid samples was analyzed using ion chromatography (Metrohm Compact IC Flex 930, The Netherlands). The equations used to analyze the mass transport and Coulombic efficiency (CE) were as follows:

$$m_A = (C_{A,i}{}^{*}V_i) - (C_{A,f}{}^{*}V_f) \tag{1}$$

$$\mathrm{CE} = \frac{\left[\frac{m_A}{N_{\mathrm{CP}}}\right]^{*} F}{M_A{}^{*}I^{*}(t_f - t_i)} \tag{2}$$

where m_A represents the mass of ion "A" transferred from the dilute to the concentrate chamber, $C_{A,i}$ and $C_{A,f}$ denote the initial and final concentrations of ion A in the dilute stream, and V_i and V_f represent the initial and final volumes of the stream. F is the Faraday's constant, N_{CP} is the number of cell pairs in the stack, M_A is the molar mass of ion A, I is the electric current applied to the ED stack, and t_f and t_i are the final and initial times.

The percentage mass recovered ($\%_{\mathrm{recovered}}$) was calculated using the following equation:

$$\%_{\mathrm{recovered}} = \frac{m_A}{C_{A,i}{}^{*}V_i} \times 100 \tag{3}$$

Energy consumption (P) and energy efficiency (EE) for acetate extraction were calculated as

$$P = \sum V^{*}I^{*}t \tag{4}$$

$$\mathrm{EE} = \frac{m_A}{P} \tag{5}$$

where V and I represent the voltage and the electric current applied to the ED stack, respectively, and t denotes the operation time.

3. RESULTS AND DISCUSSION

3.1. Effect of pH

Batch experiments (E2−4, Table 1) were conducted at a constant current density of 1.9 mA cm^{-2} to evaluate the effect of the initial solution pH (3.0, 5.5, and 7.5) on acetate (and competing ions) transport from the dilute stream to the concentrate stream. An initial pH of 3 resulted in a negligible acetate transfer toward the concentrate stream, with a concentration increase of only 0.16 ± 0.03 g L^{-1} within the 50 min duration of the experiment (Figure 2C). As an intrinsic thermodynamic property, the pK_a of a compound will determine the strength of an acid in the solution, determining the dissociation of a compound at a certain pH. The pK_a of acetic acid is 4.76; thus, in the experimental conditions of pH 3 (E2), the acetate remains mostly un-ionized (CH_3COOH), preventing its electricity-driven transport through the AEM. Thus, at pH 3.0, acetate in the dilute stream was retained, while other abundant ions (Na^+ and Cl^-) were transported, with an average percentage mass recovery of 81.48 ± 4.17% and 89.89 ± 3.70%, respectively (Figure S-1 in the Supporting Information). Since acetate was mostly un-ionized, the system reached stop conditions (dilute stream conductivity close to 1 mS cm^{-1}) when Cl^- and Na^+ were depleted, after approximately 50 min,

https://doi.org/10.1021/acsengineeringau.5c00110
ACS Eng. Au XXXX, XXX, XXX−XXX

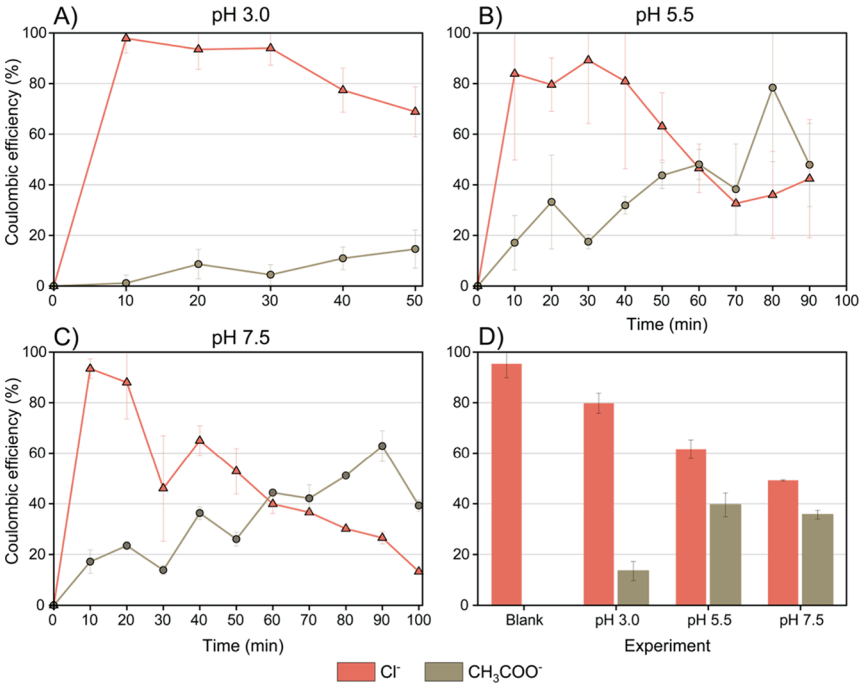

Figure 3. Effect of pH on the Coulombic efficiency (CE) for the transport of Cl^- and CH_3COO^- ions in the ED stack as a function of time at (A) pH 3.0, (B) pH5.5, and (C) pH 7.5. (D) Effect of pH on the overall CE for Cl^- and CH_3COO^- ions in the ED stack for experiments E1−E4.

like the blank experiment (Figure 2A,B) conducted in the absence of acetate.

The Coulombic efficiency (CE) was also calculated to determine how much of the electrical charge applied to the system contributed to the transport of the ions (Figure 3). At pH 3.0, the CE of Cl^- accounted, on average, for 85.31 ± 1.12%, confirming that it was the main anion transported. Of the remaining ∼15%, CH_3COO^- accounted for only 9.10 ± 1.87% while the rest of the anions in the system (PO_4^{3-}, SO_4^{2-}, and HCO_3^-) added to the remaining 6%. The efficiency of Cl^- decreased over time, as the anion was transferred from the dilute to the concentrate stream but remained above 60% throughout the experiment (Figure 3A).

When the feed solution pH was set to 5.5, acetate was successfully transferred from the dilute to the concentrate stream (Figure 2C), reaching an average concentration of 7.24 ± 0.28 g L^{-1} by the end of the experiment (around 80 min). At pH 5.5, about 70% of the acetic acid is ionized, allowing for its transport through the AEM. The CH_3COO^- concentration profiles in the concentrate and dilute chambers (Figure 2C) reveal a slow concentration variation in the first 30−40 min of operation and a progressive increase from 40 to 80 min of operation. The concentration variation of Cl^- showed an opposite trend, with a fast increase in the first 40 min of operation, and a decrease in concentration variation during the second half of the experiment (Figure 2B), suggesting competition for transport among the two anions. According to the Stokes−Einstein equation, the diffusion coefficients in aqueous solution for CH_3COO^- and Cl^- at 25 °C are $1.089 \cdot 10^{-9}$ and $2.030 \cdot 10^{-9}$ m^2 s^{-1}, respectively.[26] Considering that the initial concentrations of Cl^- (6.1 g L^{-1}) and CH_3COO^- (5.0 g L^{-1}) were similar, results suggest that when both Cl^- and CH_3COO^- are equally available, the transport of Cl^- is faster, taking most of the ion-exchange capacity of the AEM and delaying the transport of CH_3COO^-. The observed competition between Cl^- and CH_3COO^- and the increase in CH_3COO^- CE only after Cl^- is depleted agree with the results obtained by Zhang et al.[27] on the separation of organic ions from salts by ED.

The CE for Cl^- at pH 5.5 (E3) followed a similar trend than at pH 3.0 (E2) but remained lower (Figure 3A,B), with a maximum of 78.90 ± 11.42% in the early stage of the experiment and a minimum of 29.93 ± 4.57% at the later stages, resulting in an average of 57.81 ± 1.64% (Figure 3D). Concurrently, the CE for CH_3COO^- extraction increased over time to a maximum of 68.11 ± 14.73% (Figure 3B) with an overall CE of 34.98 ± 1.87% over the 80 min experiment (Figure 3D). Since the AEM used in this study exhibited no specific selectivity toward CH_3COO^- nor Cl^-, this ion transport competition is primarily linked to ion diffusivity, confirming that Cl^- transport outcompeted CH_3COO^- when the ions are present at similar concentrations.

The same trend was confirmed in E4, at an initial pH of 7.5, where both Cl^- and CH_3COO^- profiles were similar to those obtained at pH 5.5 (Figure 2B,C). However, the higher abundance of dissociated acetic acid resulted in a longer time required to reach stop conditions (around 100 min) and a higher final acetate concentration in the concentrate chamber (8.33 ± 0.52 g L^{-1}) (Figure 2C).

At pH 7.5, the overall CE of CH_3COO^- transport was 35.64 ± 1.74% (Figure 3D), with a maximum of 62.86 ± 6.09% (Figure 3C), similar to the CE achieved at pH 5.5. Again, the charge applied to the ED stack initially contributed mostly to the Cl^- transport, reaching CEs higher than 90% for this ion in the first 20 min of operation, while CH_3COO^- was mostly transported after 60 min of operation (Figure 3C).

Despite the higher concentration achieved at pH 7.5 than at pH 5.5, no significant difference in the total CE was observed (Figure 3D). Hence, considering that an extended operation time will result in high-energy consumption, pH 5.5 was selected as the best trade-off for subsequent experiments. This decision was further supported by the fact that pH 5.5 is closer to the typical pH range of MES effluents (between 4.5 and 6.0),[28,29]

https://doi.org/10.1021/acsengineeringau.5c00110
ACS Eng. Au XXXX, XXX, XXX−XXX

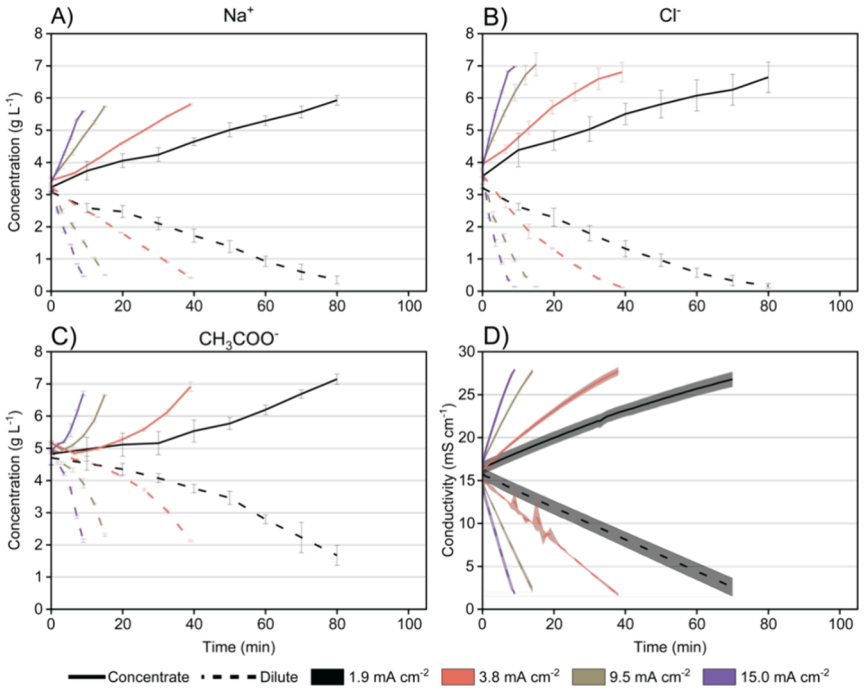

Figure 4. Effect of current density on the ion transport from the ED streams as a function of time for (A) Na^+, (B) Cl^-, and (C) CH_3COO^-. (D) Effect of the current density on the conductivity variation of the ED streams as a function of time for E5−E8.

allowing for the direct feeding of the MES outlet into the ED system with minimal to no addition of NaOH for pH adjustment.

3.2. Effect of Current Density

The effect of the operating current density was experimentally evaluated by applying 1.9 to 3.8, 9.5, and 15.0 mA cm^{-2} at an initial pH of 5.5. To enhance mixing and avoid concentration polarization at the higher current densities,[24,30] the linear flow velocity was increased from 10.2 to 30.5 cm h^{-1}, although this had only a marginal effect on ion transport (Figure S-2 in the Supporting Information).

Doubling the current density from 1.9 to 3.8 mA cm^{-2} halved the time required to reach stop conditions, from 80 to 40 min (Figure 4). This aligns with other studies stating that a higher current density allows faster ion transfer, reducing the operation time of ED systems up to a limit, dependent on the system, where side effects such as concentration polarization on the membrane-solution interface, water-splitting, or excessive voltage offset the benefits.[31] Similar concentration profiles and mass recovery (within a 10% range) were obtained at 1.9 and 3.8 mA cm^{-2} for both Na^+ (Figure S-1 in the Supporting Information) and Cl^-. However, the mass recovery of CH_3COO^- dropped from 67.08 ± 4.18 to 59.48 ± 1.03%, indicating a decrease in transport for this ion.

Further increasing the current density to 9.5 and 15.0 mA cm^{-2} led to a proportional decrease in operation time to 15 and 10 min, respectively. The mass recovery of Cl^- remained constant regardless of the current applied, suggesting that the faster transport of the ions had no significant effect on the recovery efficiency of Cl^-. Instead, the mass recovery of CH_3COO^- decreased to 57.36 ± 0.68% with 9.5 mA cm^{-2} and 58.76 ± 0.83% with 15.0 mA cm^{-2}, lower than that in the experiment at 1.9 mA cm^{-2}. This decrease in CH_3COO^- recovery efficiency can be associated with the shorter operating time of the system operating at low dilute stream conductivity, where higher transport for CH_3COO^- takes place.

The increase in current density positively affected the CE of Na^+ (Figure S-3 in the Supporting Information) and Cl^-, which increased by 10 and 15%, respectively, when the current density was raised from 1.9 and 9.5 mA cm^{-2}. Regardless of the current applied, the CE for Cl^- was the highest in the first minutes of operation, reaching values of up to 93.80 ± 13.80% (at 3.8 mA cm^{-2} applied current) before decreasing steadily until the end of the experiment.

On the other hand, an overall CE above 30% was observed for CH_3COO^- in all experiments (Figure 5E), indicating that a similar amount of the applied electric energy was used to move these ions. The different CE trends between CH_3COO^- and Cl^- ions can be attributed to differences in the transport kinetics between the two ions. Haflich et al.[32] demonstrated that, unlike Cl^-, the transport of volatile fatty acids in electrodialysis is primarily governed by ion mobility. Acetate, being less mobile and more prone to interactions with the membrane's fixed charges, experiences reduced transport rates compared to the inorganic ions in the system. Thus, the CH_3COO^- ions have less time to reach the concentrate stream at higher current densities, resulting in a lower mass recovery.

Increasing the applied current density accelerated ion transport and reduced the operational time; however, this did not necessarily translate into an improvement in acetate mass transfer. Due to their higher mobility, Cl^- and Na^+ were rapidly depleted at the highest current densities, increasing system resistance and causing an exponential rise in ED cell voltage (Figure S-4 in the Supporting Information). Additionally, higher current densities caused a rapid decrease in conductivity, quickly reaching stop conditions and limiting the time available for CH_3COO^- transport through the AEM. In fact, the CE of CH_3COO^- transport showed an inverse relationship with the conductivity (Figure 5). It increased from around 30% when the

https://doi.org/10.1021/acsengineeringau.5c00110
ACS Eng. Au XXXX, XXX, XXX−XXX

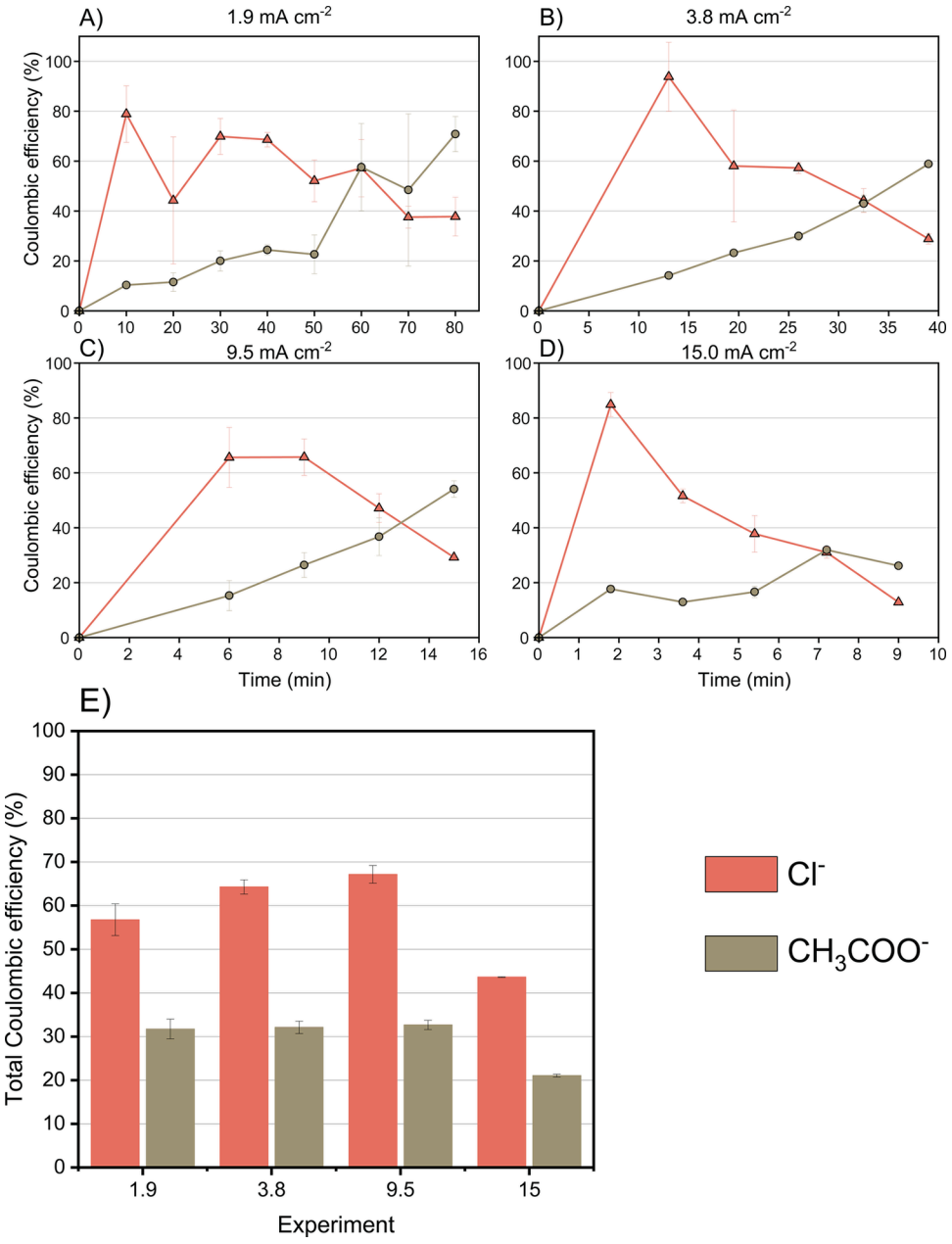

Figure 5. Effect of current density on Coulombic efficiency of the ED stack for the transport of Cl^- and CH_3COO^- ions as a function of time at (A) 1.9 mA cm^{-2}, (B) 3.8 mA cm^{-2}, (C) 9.5 mA cm^{-2}, and (D) 15.0 mA cm^{-2}. (E) Effect of current density on the total Coulombic efficiency of Cl^- and CH_3COO^- in the ED stack for experiments E5−E8.

conductivity of the dilute stream was around 8 mS cm^{-1}, up to 60% when the conductivity was in the range of 4.4−1.0 mS cm^{-1}.

The observed reduction in acetate transport CE efficiency with increasing current density aligns with the literature examples such as Dai et al.,[33] where the integration of ED with an anaerobic digestion system to separate acetate, propionate, and ethanol showed that increasing the applied current density from 14 to 36 mA cm^{-1} causes a decline in current efficiency from 51.4 to 33.8%. The present study further highlights the impact of faster ion transport on ion competition. Since higher current densities did not enhance CH_3COO^- recovery efficiency, a current density of 1.9 mA cm^{-2} was selected as the most efficient for subsequent experiments.

3.3. Effect of the Operation Mode

In the context of integrating acetate extraction into the MES cells, a key question is how the operation mode impacts the mass recovered of the system. The continuous mode allowed the dilute stream to reach a steady state. However, the low conductivity of the dilute stream at steady state may negatively impact energy consumption. The fed-batch mode combines the advantages of both batch and continuous processes. This approach enables acetate extraction when its concentration in the feed is sufficiently high, ensuring the maximum extraction rate from the dilute solution.[34]

Although both continuous and fed-batch operations exhibited a similar concentration variation rate during the first 3 h, the continuous system achieved a lower final concentration for both CH_3COO^- and Cl^- (Figure 6). By the end of the experiment

https://doi.org/10.1021/acsengineeringau.5c00110
ACS Eng. Au XXXX, XXX, XXX−XXX

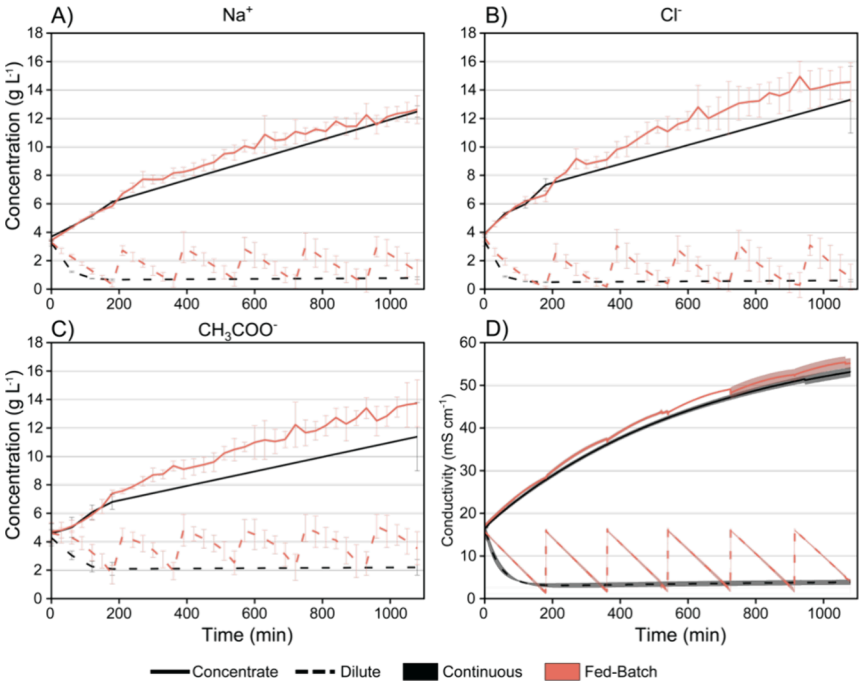

Figure 6. Comparison of ion concentration on the ED streams as a function of time under continuous and fed-batch operation for (A) Na^+, (B) Cl^-, and (C) CH_3COO^-. (D) Effect of operating mode on the conductivity variation of the ED streams as a function of time.

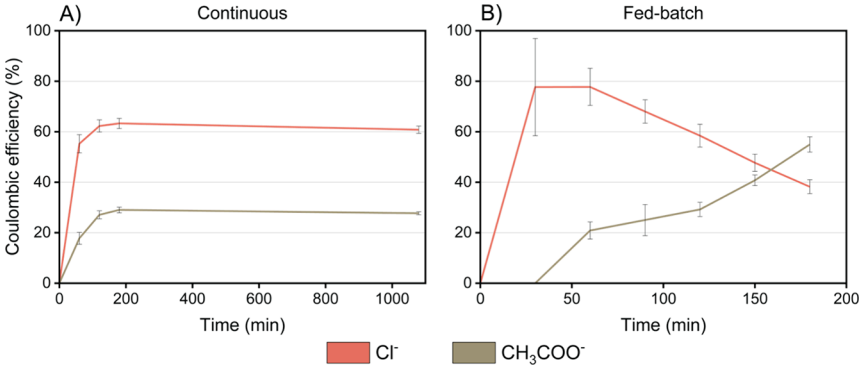

Figure 7. Effect of operating modes on the Coulombic efficiency for Cl^- and CH_3COO^- on the ED stack as a function of time for (A) continuous operation-E9 and (B) fed-batch-E10.

(18 h), the CH_3COO^- concentration in continuous mode reached 11.38 ± 2.40 g L^{-1}, whereas the fed-batch mode achieved a higher concentration of 13.73 ± 1.65 g L^{-1} (Figure 6C). This lower concentration in continuous mode can be attributed to ion loss through the outlet stream, as the dilute stream was not fully depleted of ions, and these losses must be considered. Additionally, batch experiments (E2−E8) demonstrated that CH_3COO^- concentration variation increased exponentially as conductivity decreased, reaching a maximum when dilute stream conductivity approached 1.50 mS cm^{-1}. In contrast, in continuous mode, such conditions were not attained as the dilute stream maintained a constant conductivity of 3.9 mS cm^{-1} (Figure 6D). Reducing the influent flow rate in continuous operation could allow the system to reach a lower conductivity in the dilute stream. However, this would also increase the system's voltage, requiring a trade-off between mass recovery and energy consumption.

The fed-batch mode (E10) allowed for at least 30 min of operation below the average conductivity of 3.9 mS cm^{-1} observed in continuous mode (Figure 6D), facilitating more efficient CH_3COO^- transport and enabling the recovery of over 30% of the available mass.

In continuous mode, the CE of Cl^- peaked within the first 200 min, reaching 63.29 ± 1.99%, and then plateaued (Figure 7A). Since the conductivity of the dilute stream never fell below 2 mS cm^{-1}, Cl^- transport consistently outcompeted CH_3COO^- transport throughout the experiment, with average CE values of 60.40 ± 3.11% for Cl^- and 25.40 ± 4.45% for CH_3COO^-. Figure 7B presents the average CE values for Cl^- and CH_3COO^- across six batches. Results indicate a higher CE for CH_3COO^- in the final 60 min of each batch, compared to the average CE in continuous operation, reaching a maximum of 54.98 ± 3.05% across all batches. This efficiency corresponds to the low-conductivity region attained in all batches (Figure 6D), confirming that the maximum CE of CH_3COO^- and thus its highest transport occur at the end of each batch.

Comparisons between ED operating modes were conducted in previous studies. Wang et al.[35] evaluated ED performance for phosphate recovery in both batch and continuous modes, achieving near-complete recovery in batch mode and 95.8%

https://doi.org/10.1021/acsengineeringau.5c00110
ACS Eng. Au XXXX, XXX, XXX−XXX

Table 2. Electric Power Consumption and Recovery Efficiency in the Experiments Performed. All the values represent the average and standard deviation of triplicates

					average final conductivity (mS cm^{-1})	
experiment	average voltage (V)	energy consumed (Wh)	average final CH_3COO^- (g L^{-1})	recovery efficiency (kg kWh^{-1})	concentrate	dilute
E2	3.01 ± 0.30	0.52 ± 0.04	4.52 ± 0.22	0.17 ± 0.10	19.78 ± 0.04	1.89 ± 0.27
E3	3.02 ± 0.36	0.76 ± 0.01	7.24 ± 0.28	1.14 ± 0.03	26.16 ± 0.48	1.47 ± 0.24
E4	2.98 ± 0.37	0.91 ± 0.03	8.33 ± 0.52	1.15 ± 0.19	29.15 ± 0.16	1.29 ± 0.05
E5	2.61 ± 0.29	0.66 ± 0.04	7.15 ± 0.16	1.26 ± 0.12	26.78 ± 0.88	1.86 ± 0.22
E6	3.35 ± 0.41	0.85 ± 0.04	6.91 ± 0.15	0.74 ± 0.06	27.74 ± 0.47	1.69 ± 0.15
E7	4.83 ± 0.75	1.18 ± 0.08	6.65 ± 0.02	0.49 ± 0.02	27.75 ± 0.26	2.01 ± 0.30
E8	6.11 ± 1.22	1.45 ± 0.06	6.70 ± 0.07	0.35 ± 0.01	27.93 ± 0.05	1.80 ± 0.05
E9	3.36 ± 0.28	11.65 ± 0.14	11.39 ± 2.41	0.80 ± 0.23	53.10 ± 1.14	4.21 ± 0.26
E10	2.95 ± 0.26	10.41 ± 0.28	13.73 ± 1.65	1.12 ± 0.03	55.17 ± 1.17	2.10 ± 0.90

recovery in the continuous mode. In their study, the higher performance of the batch system was attributed to the longer operating time. Similarly, Jones et al.[36] used continuous ED to separate VFA's from a bioreactor, successfully increasing the acetic acid concentration from 0.01 to 2.70 g L^{-1}. Comparing these ED systems remains challenging due to differences in current densities and target compounds across studies. However, both authors emphasize that in continuous operation, residual target compounds remain in the dilute stream, preventing full recovery. In the present study, the superior performance of the fed-batch system was attributed to prolonged operation at low conductivity, which enhanced CH_3COO^- transport over Cl^-. However, considering the overall process, the fed-batch system exhibited an average conductivity of 8.87 mS cm^{-1}, whereas the continuous system maintained a lower average conductivity of 3.9 mS cm^{-1}. The higher conductivity in the fed-batch mode was advantageous for energy efficiency, resulting in a lower ED cell voltage for most of the operation (Figure S-4 in the Supporting Information).

3.4. Energy Consumption and Recovery

Minimizing energy consumption is a key objective in the application of ED as a separation step.[37] As shown in Table 2, batch experiments conducted at an applied current of 1.9 mA cm^{-2} and a pH of either 5.5 or 7.5 (E3, E4, and E5) achieved the highest recovery per unit of electric energy invested, ranging from 1.14 to 1.26 kg kWh^{-1}. This indicates that these conditions provided the best balance between the energy input and recovery efficiency. The variation in pH throughout the operation of these experiments is presented in Figure S-5 of the Supporting Information.

The fed-batch system achieved 16% higher final acetate concentration and 11% lower energy consumption compared to the continuous mode, resulting in a higher acetate recovery efficiency of 1.12 ± 0.03 kg kWh^{-1} (Table 2). The higher electrical power demand in continuous mode was attributed to the consistently low conductivity of the dilute stream, resulting in a higher average cell voltage throughout the operation. In contrast, the fed-batch mode experienced periodic increases in conductivity when the dilute was replenished, which reduced the system's resistance, lowered the average voltage, and ultimately decreased energy consumption.

Different strategies have been proposed for recovery of acetic acid from the MES electrolyte. Traditional methods such as solvent extraction or distillation are not sustainable as they introduce solvents or high-energy costs to an already energy-consuming and sensible process, where the initial acetate concentration is typically low.[38] Since the operation pH of MES systems is often above the acetic acid pK_a, technology based on ion separation, such as membranes or resins are preferable for product recovery.[39,40] *In situ* methods, integrating production and extraction in the same cell, mitigate issues such as product inhibition, but complicate operation and inevitably adds ohmic resistance to the system, increasing the energy expenses.[16] *Ex situ* methods, integrating MES with downstream product recovery offers a high level of maturity and energy efficiency, making it attractive for integration with MES processes where energy efficiency remains a central constraint for.[22,39]

Based on previously reported acetate productivity values of 0.04 kg kWh^{-1} in MES systems,[23] it is estimated that a 2.5-fold increase in acetate concentration using ED as presented in this work would require only ∼5% of the total energy demand for MES production. Information on energy consumption for acetate production and extraction in MES is scarce. Gadkari et al.[41] assessed the energy requirements of an extractive distillation unit combined with an acetic acid-producing MES system through life cycle assessment (LCA). Regardless of the different scenarios applied, distillation led to at least 80% of the overall energy consumption of the process (10.5 kWh per kilogram of acetic acid in their best-case scenario). Jourdin et al.[42] also developed a techno-economic analysis of MES systems including the downstream stage, setting a maximum purification value that any extraction stage would have to achieve to reach economic feasibility. Both authors agree that conventional downstream technologies with high-energy demands, such as distillation, are not economically sustainable for purifying diluted streams from MES. Thus, efficient, less energy-intensive technologies are required for scaled MES systems.

While the final acetic acid concentration achieved in this work remains insufficient for industrial applications, vinegar production could be a potential use for the concentrated products.[43] Additional concentration steps are necessary to reach broader applications. Future research should focus on the development of ion-selective membranes[44] or the use of multistage ED setups such as the one proposed by Shi et al.,[45] which successfully increased VFA concentration from 15 to 90%, demonstrating the potential of such configurations to overcome limitations of ion competition, reaching higher final titers.

Long-term studies to test the performance of the membranes can help assess potential issues such as scaling or degradation. A broader comparison of ED with other separation technologies applied to MES product recovery is also required to further evaluate the integration of the MES-ED systems.

https://doi.org/10.1021/acsengineeringau.5c00110
ACS Eng. Au XXXX, XXX, XXX−XXX

4. CONCLUSIONS

This study demonstrates the potential of ED as a downstream separation process for recovery of acetate from a simulated MES effluent. Operating at pH values above the pK_a of the target compound facilitated its ionization, enabling its electricity-driven transport through the ED system. Operating in fed-batch mode allowed the system to reach conditions favorable for acetate transport. While high current densities reduced operating time, they intensified ion competition with Cl^-, increasing energy consumption and limiting the CE of acetate transport. The highest acetate concentration in the concentrate stream was achieved with a pH of 5.5 in the feed solution, applying 1.9 mA cm^{-2} in the fed-batch operation. This yielded a final recovery efficiency of 55.47 ± 6.35%, achieving a concentration of 13.73 ± 1.65 g L^{-1} in the concentrate solution. On average, 1.12 kg of acetate was recovered per kWh^{-1} of electric energy invested.

This study provides guidance on how different operating parameters and competing ions commonly found in MES affect the ED efficiency of ED. The results identify ED as a low energy-consuming process, a key requirement for decreasing the energy expenses and increasing the economic feasibility of MES at large scale.

■ ASSOCIATED CONTENT

Supporting Information

The Supporting Information is available free of charge at https://pubs.acs.org/doi/10.1021/acsengineeringau.5c00110.

Mass recovery results, linear flow velocity comparison, Na^+ Coulombic efficiency, voltage variation, pH variation (PDF)

■ AUTHOR INFORMATION

Corresponding Author

Santiago Martínez Sosa − *School of Biological and Chemical Sciences, Ryan Institute, University of Galway, Galway H91 CF50, Ireland;* orcid.org/0000-0003-2187-210X; Email: s.martinezsosa1@universityofgalway.ie

Authors

Qingdian Shu − *Wetsus, European Centre of Excellence for Sustainable Water Technology, Leeuwarden MA 8911, The Netherlands;* orcid.org/0000-0001-5454-8053

Michele Tedesco − *TNO Sustainable Processes and Energy Systems, Rijswijk 2288 GJ, The Netherlands;* orcid.org/0000-0002-3389-5168

Hubertus V.M. Hamelers − *Wetsus, European Centre of Excellence for Sustainable Water Technology, Leeuwarden MA 8911, The Netherlands; Environmental Technology, Wageningen University & Research, Wageningen 6708WG, The Netherlands*

Pau Farràs − *School of Biological and Chemical Sciences, Ryan Institute, University of Galway, Galway H91 CF50, Ireland;* orcid.org/0000-0003-3859-2868

Paolo Dessì − *Department of Agricultural Sciences, University of Naples Federico II, Campania 80055, Italy*

Complete contact information is available at: https://pubs.acs.org/10.1021/acsengineeringau.5c00110

Author Contributions

Santiago Martínez Sosa: conceptualization, investigation, writing (original draft), funding acquisition. Qingdian Shu: methodology, writing (review and editing), visualization, validation, investigation, conceptualization. Paolo Dessì: methodology, visualization, writing (review and editing). Michele Tedesco: writing (review and editing). Hubertus V.M. Hamelers: writing (review and editing). Pau Farras: conceptualization, supervision, project administration, funding acquisition, writing (review and editing).

Notes

The authors declare no competing financial interest.

■ ACKNOWLEDGMENTS

The research conducted in this publication was funded by the Irish Research Council under grant number GOIPG/2022/2272 on the project "Design of a scalable microbial electrosynthesis cell for the efficient industrial CO_2 recycling".

■ REFERENCES

(1) Agboola, M. O.; Bekun, F. V.; Joshua, U. Pathway to environmental sustainability: Nexus between economic growth, energy consumption, CO2 emission, oil rent and total natural resources rent in Saudi Arabia. *Resources Policy* **2021**, *74*, No. 102380.

(2) *Climate Change: Atmospheric Carbon Dioxide*. NOAA Climate.gov. Accessed: Feb. 08, 2024. https://www.climate.gov/news-features/understanding-climate/climate-change-atmospheric-carbon-dioxide#.

(3) Nocito, F.; Dibenedetto, A. Atmospheric CO2 mitigation technologies: carbon capture utilization and storage. *Curr. Opin. Green Sustain. Chem.* **2020**, *21*, 34−43.

(4) United Nations/Framework Convention on Climate Change. The Paris Agreement. In *Adoption of the Paris Agreement*; UNFCCC: Paris, 2015. Accessed: Mar. 19, 2024. https://unfccc.int/process-and-meetings/the-paris-agreement.

(5) Di Maio, F.; Rem, P. C. A Robust Indicator for Promoting Circular Economy through Recycling. *J. Environ. Prot.* **2015**, *6* (10), 1095−1104.

(6) Anastas, P. T.; Warner, J. C. *Green Chemistry: Theory and Practice*; Oxford University Press, **2000**. .

(7) Boucher, D. G.; et al. Bioelectrocatalytic Synthesis: Concepts and Applications. *Angew. Chem.* **2023**, *135* (46), No. e202307780.

(8) Rabaey, K.; Rozendal, R. A. Microbial electrosynthesis — revisiting the electrical route for microbial production. *Nature Reviews Microbiology* **2010**, *8* (10), 706−716.

(9) Vogt, E. T. C; Weckhuysen, B. M. The refinery of the future. *Nature* **2024**, *629*, 295.

(10) Cuellar, M. C.; Straathof, A. J. Downstream of the bioreactor: advancements in recovering fuels and commodity chemicals. *Curr. Opin. Biotechnol.* **2020**, *62*, 189−195.

(11) Jiang, Y.; Zeng, R. J. Expanding the product spectrum of value added chemicals in microbial electrosynthesis through integrated process design—A review. *Bioresour. Technol.* **2018**, *269*, 503−512.

(12) Freeman, A.; Woodley, J. M.; Lilly, M. D. In situ product removal as a tool for bioprocessing. *Biotechnology (N Y).* **1993**, *11* (9), 1007−1012.

(13) Murali, N.; Srinivas, K.; Ahring, B. K. Biochemical Production and Separation of Carboxylic Acids for Biorefinery Applications. *Fermentation* **2017**, *3* (2), 22.

(14) Saboe, P. O.; et al. In situ recovery of bio-based carboxylic acids. *Green Chem.* **2018**, *20* (8), 1791−1804.

(15) Matemadombo, F.; et al. Modelling the simultaneous production and separation of acetic acid from CO2 using an anion exchange membrane microbial electrosynthesis system. *J. Chem. Technol. Biotechnol.* **2017**, *92* (6), 1211−1217.

(16) Gildemyn, S.; Verbeeck, K.; Slabbinck, R.; Andersen, S. J.; Prévoteau, A.; Rabaey, K. Integrated production, extraction, and

concentration of acetic acid from CO2 through microbial electrosynthesis. *Environ. Sci. Technol. Lett.* **2015**, *2* (11), 325−328.
(17) Li, Q. Z.; et al. Recovery Processes of Organic Acids from Fermentation Broths in the Biomass-Based Industry. *J. Microbiol. Biotechnol.* **2016**, *26* (1), 1−8.
(18) Zhou, R.; et al. Revisiting bipolar membrane electrodialysis for the production of monoprotic organic acids with different pKa and Mw. *Chemical Engineering Journal* **2025**, *505*, No. 159125.
(19) Suwal, S.; Li, J.; Engelberth, A. S.; Huang, J. Y. Application of electro-membrane separation for recovery of acetic acid in lignocellulosic bioethanol production. *Food and Bioproducts Processing* **2018**, *109*, 41−51.
(20) Jones, R. J.; Massanet-Nicolau, J.; Guwy, A.; Premier, G. C.; Dinsdale, R. M.; Reilly, M. Removal and recovery of inhibitory volatile fatty acids from mixed acid fermentations by conventional electrodialysis. *Bioresour. Technol.* **2015**, *189*, 279−284.
(21) Pan, S. Y.; Gianto, J. M.; Lin, Y. I.; Chang, H. M. Advancing water and resource recovery from brackish water through electrodialysis-based technologies for circular product ecosystems. *Desalination* **2026**, *619*, No. 119550.
(22) Pan, Z.; et al. Coupling electrodialysis with microbial electrosynthesis enables high-rate, high-titer, and cost-effective acetate production from CO2. *Bioresour. Technol.* **2025**, *424*, No. 132280.
(23) Dessì, P.; et al. Microbial electrosynthesis of acetate from CO2 in three-chamber cells with gas diffusion biocathode under moderate saline conditions. *Environmental Science and Ecotechnology* **2023**, *16*, No. 100261.
(24) Tanaka, Y. *Ion Exchange Membranes: Fundamentals and Applications*, Second Edition; Elsevier, **2015**, pp 1−500. .
(25) Abdel-Ghafar, H. M.; Abdel-Aal, E. A.; El-Sayed, D.; Hoinkis, J. Optimization of electrodialysis unit for partial desalination: Batch and continuous operation. *Appl. Chem. Eng.* **2021**, *4* (1), 1−8.
(26) *Table of Diffusion Coefficients*. Accessed: Feb. 29, 2024. https://www.aqion.de/site/diffusion-coefficients.
(27) Zhang, Y.; Pinoy, L.; Meesschaert, B.; Van der Bruggen, B. Separation of small organic ions from salts by ion-exchange membrane in electrodialysis. *AIChE J.* **2011**, *57* (8), 2070−2078.
(28) Ziara, R. M. M.; Miller, D. N.; Subbiah, J.; Dvorak, B. I. Lactate wastewater dark fermentation: The effect of temperature and initial pH on biohydrogen production and microbial community. *Int. J. Hydrogen Energy* **2019**, *44* (2), 661−673.
(29) Jourdin, L.; Grieger, T.; Monetti, J.; Flexer, V.; Freguia, S.; Lu, Y.; Chen, J.; Romano, M.; Wallace, G. G.; Keller, J. High Acetic Acid Production Rate Obtained by Microbial Electrosynthesis from Carbon Dioxide. *Environ. Sci. Technol.* **2015**, *49* (22), 13566−13574.
(30) Belfort, G.; Guter, G. A. An experimental study of electrodialysis hydrodynamics. *Desalination* **1972**, *10* (3), 221−262.
(31) Nagarale, R. K.; Gohil, G. S.; Shahi, V. K.; Trivedi, G. S.; Thampy, S. K.; Rangarajan, R. Studies on transport properties of short chain aliphatic carboxylicacids in electrodialytic separation. *Desalination* **2005**, *171* (2), 195−204.
(32) Haflich, H. M.; Singleton, J. W.; Coronell, O. Relative contributions of mobility and partitioning to volatile fatty acid flux during electrodialysis. *J. Membr. Sci.* **2024**, *711*, No. 123204.
(33) Dai, K.; et al. Impacts of medium composition and applied current on recovery of volatile fatty acids during coupling of electrodialysis with an anaerobic digester. *J. Clean. Prod.* **2019**, *207*, 483−489.
(34) Campione, A.; Gurreri, L.; Ciofalo, M.; Micale, G.; Tamburini, A.; Cipollina, A. Electrodialysis for water desalination: A critical assessment of recent developments on process fundamentals, models and applications. *Desalination* **2018**, *434*, 121−160.
(35) Wang, X.; Wang, Y.; Zhang, X.; Feng, H.; Li, C.; Xu, T. Phosphate recovery from excess sludge by conventional electrodialysis (CED) and electrodialysis with bipolar membranes (EDBM). *Ind. Eng. Chem. Res.* **2013**, *52* (45), 15896−15904.
(36) Jones, R. J.; Fernández-Feito, R.; Massanet-Nicolau, J.; Dinsdale, R.; Guwy, A. Continuous recovery and enhanced yields of volatile fatty acids from a continually-fed 100 L food waste bioreactor by filtration and electrodialysis. *Waste Management* **2021**, *122*, 81−88.
(37) Patel, S. K.; Qin, M.; Walker, W. S.; Elimelech, M. Energy Efficiency of Electro-Driven Brackish Water Desalination: Electrodialysis Significantly Outperforms Membrane Capacitive Deionization. *Environ. Sci. Technol.* **2020**, *54* (6), 3663−3677.
(38) Prévoteau, A.; Carvajal-Arroyo, J. M.; Ganigué, R.; Rabaey, K. Microbial electrosynthesis from CO2: forever a promise? *Curr. Opin. Biotechnol.* **2020**, *62*, 48−57.
(39) Bajracharya, S.; et al. In situ acetate separation in microbial electrosynthesis from CO2 using ion-exchange resin. *Electrochim. Acta* **2017**, *237*, 267−275.
(40) Pal, P.; Nayak, J. Acetic Acid Production and Purification: Critical Review Towards Process Intensification. *Separation and Purification Reviews* **2017**, *46* (1), 44−61.
(41) Gadkari, S.; Mirza Beigi, B. H.; Aryal, N.; Sadhukhan, J. Microbial electrosynthesis: is it sustainable for bioproduction of acetic acid? *RSC Adv.* **2021**, *11* (17), 9921−9932.
(42) Jourdin, L.; Sousa, J.; van Stralen, N.; Strik, D. P. B. T. B. Techno-economic assessment of microbial electrosynthesis from CO2 and/or organics: An interdisciplinary roadmap towards future research and application. *Appl. Energy* **2020**, *279*, No. 115775.
(43) *Acetic acid: general information* - GOV.UK. Accessed: Feb. 25, 2025. https://www.gov.uk/government/publications/acetic-acid-properties-uses-and-incident-management/acetic-acid-general-information.
(44) Kim, N.; Lee, J.; Su, X. Precision Tuning of Highly Selective Polyelectrolyte Membranes for Redox-Mediated Electrochemical Separation of Organic Acids. *Adv. Funct. Mater.* **2023**, *33* (12), No. 2211645.
(45) Shi, L.; Hu, Y.; Xie, S.; Wu, G.; Hu, Z.; Zhan, X. Recovery of nutrients and volatile fatty acids from pig manure hydrolysate using two-stage bipolar membrane electrodialysis. *Chemical Engineering Journal* **2018**, *334*, 134−142.

https://doi.org/10.1021/acsengineeringau.5c00110
ACS Eng. Au XXXX, XXX, XXX−XXX